NextGen Scientific Publication
American International Journal of Computer Science and Technology
Volume 2 Issue 1, Pg. No. 1-11, AIJCST-V2I1P101, 2020
https://doi.org/10.63282/3117-5481/AIJCST-V2I1P101

Original Article

AI-Powered Optimization of Networked Computing Infrastructures for Low-Latency Data Processing

*** Dr. Bastin Thiyagaraj**
Department of IT, St. Joseph's College (Autonomous), Tiruchirappalli, Tamil Nadu, India.

Abstract:

Modern applications from real-time analytics to cyber-physical control demand millisecond-level responsiveness across heterogeneous, networked infrastructures. This paper presents an AI-driven optimization stack that jointly orchestrates compute, network, and data paths to minimize end-to-end latency under dynamic workloads. We model the system as a constrained Markov decision process and employ reinforcement learning for SLO-aware autoscaling, operator placement, and flow steering across edge cloud tiers. A complementary learning-to-rank scheduler prioritizes critical microservices using online features (queue depths, p95 latency, tail-loss risk) derived from kernel-level telemetry. To shrink inference delays, we integrate model-aware compilation and compression (quantization/distillation) with zero-copy data planes and adaptive batching. Network latency is reduced via intent-based routing that couples RL policies with programmable switches for congestion- and jitter-aware path selection. A control-theoretic safety layer enforces stability and cost caps, while a digital-twin emulator enables fast policy evaluation before deployment. Prototype implementation across containerized clusters demonstrates consistent reductions in tail latency and recovery time during bursty and faulted conditions, with improvements driven by closed-loop decisions rather than static heuristics. The framework is modular, explainable via attribution on scheduling actions, and portable to diverse hardware. We conclude with guidelines for production roll-out and discuss open challenges in cross-layer observability and multi-tenant fairness.

Keywords:

Edge Computing, Low-Latency Orchestration, Reinforcement Learning, Operator Placement, Slo-Aware Autoscaling, Intent-Based Networking, Kernel-Level Telemetry, Model Compression, Stream Processing, Digital Twin.

Article History:

Received: 15.11.2019

Revised: 16.12.2019

Accepted: 20.12.2019

Published: 03.01.2020

1. Introduction

The proliferation of latency-sensitive services autonomous perception, immersive analytics, industrial control, and fraud interdiction has exposed the limitations of traditional, centrally orchestrated clouds. Data now originates at the edge in micro-bursts and streams that must be acted on within tens of milliseconds, while workloads fluctuate unpredictably with user mobility, diurnal cycles, and fault transients. Conventional rule-based autoscaling and static operator placement struggle to keep pace with these dynamics, often optimizing average utilization at the expense of tail latency and stability. Meanwhile, network conditions (congestion, jitter, microbursts) and data-path inefficiencies (copy overheads, suboptimal batching) compound end-to-end delays, making holistic, cross-layer coordination indispensable.

This paper addresses the problem of low-latency data processing over heterogeneous, networked infrastructures by introducing an AI-powered optimization stack that jointly reasons about compute, network, and data flows. The core idea is to replace brittle heuristics with learning-driven decisions: reinforcement learning for SLO-aware autoscaling and operator placement; online learning-to-rank for fine-grained scheduling; and intent-based routing for congestion-aware path selection. To shrink inference and transport delays, the stack couples model compression with zero-copy data planes and adaptive batching, while a safety layer grounded in control theory enforces stability, fairness, and cost bounds. A digital-twin emulator enables rapid, risk-controlled policy iteration prior to deployment.

Our contributions are threefold: (i) a cross-layer optimization framework that converts latency objectives into actionable controls spanning edge cloud tiers; (ii) a practical design integrating kernel-level telemetry, programmable networking, and model-aware compilation to minimize tail latency; and (iii) an empirical evaluation demonstrating robust reductions in p95/p99 latency and recovery time under bursty loads and injected faults. Collectively, these results chart a path toward dependable, explainable, and cost-effective low-latency infrastructures.

2. Related Work

2.1. AI in Networked Computing

AI has progressively shifted from an application-layer add-on to a first-class orchestration primitive in networked systems. Early efforts used supervised learning for traffic classification and congestion prediction, feeding insights into fixed control loops. Subsequent work explored reinforcement learning (RL) to close the loop, mapping observed states queue depths, flow deadlines, and link utilization to actions such as rate limiting, priority assignment, and path selection. In datacenter fabrics, learned policies have been shown to outperform hand-tuned congestion control and flow scheduling by reacting to microbursts faster than threshold rules. At the edge cloud continuum, RL has been applied to service placement and migration, adapting to mobility and volatile radio conditions, while multi-armed bandits guide online configuration of caching, codec choices, and batch sizes.

Beyond control, AI assists observability: representation learning on telemetry streams (eBPF/KProbes, switch counters, application traces) extracts low-dimensional, predictive features for anomaly detection and capacity planning. GNN-based models capture topology-aware interactions (e.g., coflow dependencies), and meta-learning accelerates policy transfer across clusters with different traffic mixes. However, safety and stability remain open issues; many approaches retrofit cost constraints post hoc rather than embedding them into the learning objective, leading to occasional SLO regressions under distribution shift.

2.2. Low-Latency Data Processing Techniques

Low-latency designs historically relied on architectural choices: in-memory dataflow engines, operator fusion, and lock-free queues to minimize context switches and cache misses. Zero-copy messaging (DPDK, io_uring), kernel-bypass RPC, and user-space TCP variants reduced syscall overhead and jitter. Stream processors introduced punctuations, watermarks, and backpressure to bound queues and control out-of-order processing, while micro-batching and adaptive batching balanced amortization benefits against tail inflation.

At the model layer, quantization, pruning, and knowledge distillation have cut inference time on CPUs/NPUs without unacceptable accuracy loss, complemented by graph-level optimizations (operator folding, tensor layout rewrites). Networking advances P4-programmable switches, ECN/ECT(1) tweaks, and deadline-aware scheduling shrink queuing delay, whereas multi-path transport with coupling constraints mitigates head-of-line blocking. Recent systems push compute to the first routable hop (in-network aggregation, sketches), and co-design data paths with runtime schedulers so that queue disciplines reflect application deadlines. The persistent challenge is coordinating these techniques across layers; gains in one layer can be offset elsewhere unless controls are jointly optimized.

2.3. Optimization Approaches for Distributed Systems

Optimization for distributed systems spans exact, approximate, and learning-based methods. Classical formulations cast placement, routing, and scaling as mixed-integer or convex programs with latency and budget constraints. While optimal for small instances, they struggle with NP-hard combinatorics and non-stationarity. Heuristics (greedy bin-packing, tabu search, simulated annealing) improve tractability but can be brittle under workload churn. Queueing-theoretic models (M/M/k, G/G/1 with priorities)

provide insight into stability and tail behavior, informing control-theoretic policies (PID/LQR/SMC) that deliver provable bounds when system dynamics are well identified.

Learning-based optimization addresses scale and uncertainty by adapting policies online. RL and contextual bandits optimize long-horizon SLOs with partial observability; imitation learning distills expert traces into fast policies; and Bayesian optimization tunes high-cost knobs (e.g., JVM, NUMA, batch size) with few trials. Hybrid approaches are emerging: differentiable relaxations enable end-to-end training for placement; bilevel schemes use solvers to generate labels for supervisors; and safe RL layers enforce constraints using Lyapunov critics or control barrier functions. The consensus across strands is that no single optimizer suffices effective systems blend model-based structure for safety with data-driven adaptation for performance, underpinned by rich telemetry and fast what-if evaluation (simulators/digital twins).

3. System Architecture

3.1. Overview of the Networked Infrastructure

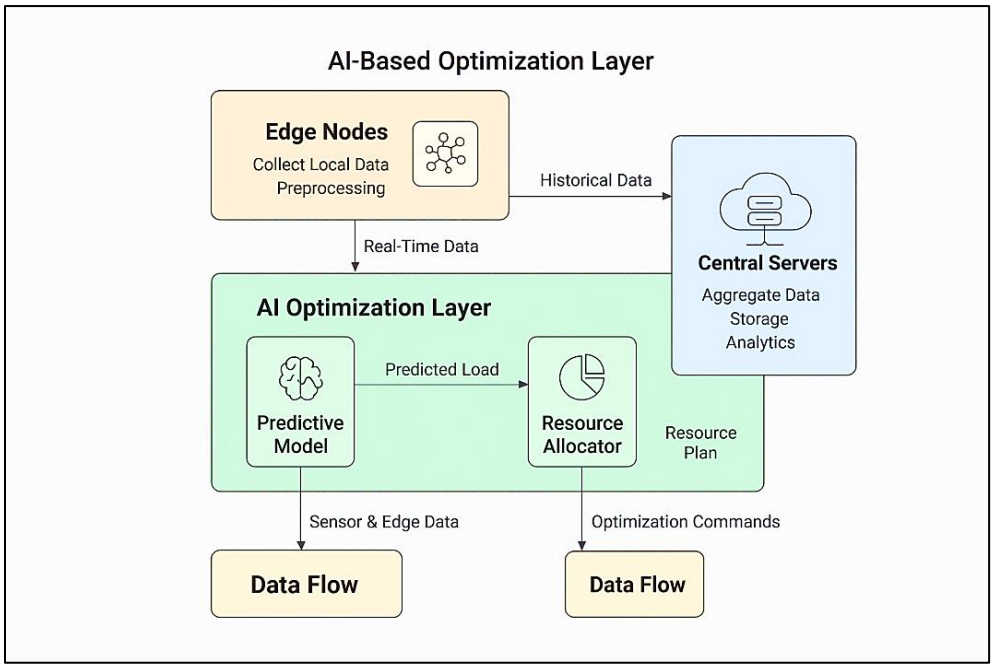

Figure 1. AI-Based Optimization Layer for Low-Latency Edge Cloud Data Processing

The figure presents a layered view of a networked edge cloud system in which an AI Optimization Layer orchestrates compute and data movement to achieve low latency. Edge nodes ingest sensor streams, perform lightweight preprocessing, and emit real-time telemetry upward. In parallel, central servers aggregate historical traces and maintain durable storage and analytics, supplying the AI layer with long-horizon context about workload seasonality, failure patterns, and capacity envelopes. This dual feed live signals from the edge and historical context from the core allows the optimizer to reason over both immediate conditions and learned trends.

Within the AI Optimization Layer, a predictive model forecasts near-term load, queue growth, and tail-latency risk using features derived from sensor data, edge metrics, and prior episodes. The forecast informs a resource allocator that produces a concrete plan: microservice placement across edge and central tiers, batch/window sizing, and rate limits or priority classes for flows. By coupling prediction with allocation, the system avoids reactive thrashing and instead proactively positions compute and network paths where they will minimize end-to-end delay.

The outputs of the allocator are emitted as optimization commands back to the infrastructure, closing the loop. Edge nodes adjust operators and buffering; the central servers reshape storage and analytics tasks; and data flows are steered along paths consistent with the plan. The same loop feeds back fresh telemetry, enabling continuous refinement of the predictive model and allocator decisions as conditions evolve (e.g., bursts, mobility, or partial failures).

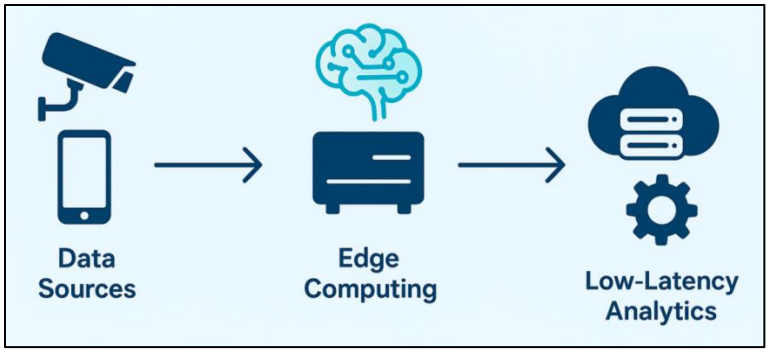

Figure 2. Data Sources Edge Computing Low-Latency Analytics Pipeline

3.2. Edge and Cloud Components

Edge tier. Edge nodes are lightweight compute appliances (x86/ARM SBCs, GPU/TPU/NPUs where available) colocated with sensors and actuators. They run a slim runtime (e.g., containerd/K3s) with sandboxed microservices for preprocessing: filtering, compression, schema validation, feature extraction, and privacy-preserving transforms (tokenization, on-device aggregation). A local cache and short-retention message log absorb jitter and enable replay after transient faults. Fine-grained telemetry is exported via eBPF/KProbes and hardware counters (CPU, NIC, accelerator), yielding per-operator latency, queue depth, and drop metrics. Because power and connectivity fluctuate, the edge stack supports opportunistic offload, graceful degradation, and fast cold-start via prewarmed containers or WASM modules.

Cloud/core tier. Central servers provide durable storage (object + columnar lakehouse), batch/stream analytics, and control-plane services. They host heavier models, global schedulers, and historical observability (time-series, traces, logs) used for capacity planning and policy learning. Multi-region clusters expose placement zones (edge PoPs, regional DCs, backbone hubs) with heterogeneous accelerators. The core also terminates cross-tenant isolation, admission control, and cost governance; it maintains the digital twin that replays real traces and "what-if" scenarios to validate policies before rollout. Together, edge and cloud form a continuum where operators can be migrated, replicated, or fused to meet latency SLOs and resilience targets.

3.3. Data Flow and Communication Protocols

Streaming and control planes. The data plane moves sensor streams and intermediate features using lightweight, backpressure-aware messaging (gRPC/HTTP-3 over QUIC for RPCs; MQTT/AMQP for constrained devices; Kafka/Pulsar for high-throughput fan-in). Watermarks and event-time semantics bound out-of-order processing; micro-batch and adaptive batching are applied when amortization beats per-event latency. Control messages placement updates, rate limits, and policy deltas travel on a separate, reliable channel with priority scheduling to ensure decisions are enacted promptly even under congestion.

Resilience, security, and timing. End-to-end mTLS with mutual authentication secures all paths; lightweight envelope encryption protects sensitive payloads crossing administrative domains. Exactly-once or effectively-once semantics are achieved with idempotent producers, transactional sinks, and replayable logs at the edge. Deadline-aware queue disciplines (priority/FIFO hybrids) and ECN/ECT(1) marking reduce tail inflation; in industrial settings, TSN (Time-Sensitive Networking) can pin deterministic flows. Schema registries and Protobuf/Avro contracts keep interfaces evolvable, while observability headers (trace IDs, causal context) enable cross-layer tracing from device to cloud.

3.4. AI-Based Optimization Layer

Prediction and decision core. The optimization layer ingests live telemetry and historical traces to forecast short-horizon load, queue growth, and tail-latency risk. Temporal models (e.g., TFT/LSTM with exogenous features, or lightweight online regressors at the edge) produce per-operator demand and contention estimates. These forecasts feed a resource allocator that solves a constrained placement/routing/scaling problem: where to execute each operator (edge vs. regional vs. core), how much compute to allocate, which batch/window sizes to use, and which paths to steer traffic along. Reinforcement learning (e.g., PPO with safety critics) handles non-stationarity, while learning-to-rank schedulers prioritize flows by predicted deadline miss risk.

Safety, explainability, and deployment loop. A control-theoretic guardrail enforces stability and cost caps using Lyapunov or barrier-function constraints; when confidence drops, the system falls back to safe heuristics. The digital twin accelerates policy iteration: candidate policies are evaluated on trace-driven simulations with fault injection before staged rollout (canary region global). Shapley/attribution analyses on scheduling actions and "what-if" counterfactuals explain decisions to operators and auditors, supporting multi-tenant fairness. Continuous learning closes the loop new traces update the predictor, while policy gradients are refreshed from real-world rewards yielding an optimizer that adapts to bursts, topology changes, and hardware heterogeneity without sacrificing SLOs.

4. Methodology / Proposed Approach

Our approach couples learning-based controllers with lightweight analytics and fast heuristics so the system can (i) anticipate demand, (ii) decide cross-layer actions, and (iii) enact them safely under tight latency SLOs. The pipeline runs continuously: telemetry from edge nodes, switches, and services is featurized; short-horizon forecasts are produced; an RL policy proposes placement, scaling, and routing moves; and a heuristic post-processor refines those moves to respect hard constraints (capacity, affinity, regulatory boundaries). A safety wrapper enforces stability via control-theoretic constraints and triggers fallbacks when uncertainty or drift is detected. Below we detail the models that realize each stage.

4.1. AI Models and Algorithms Used

We use a two-time-scale design. Fast, online predictors operate per node/flow at millisecond second cadence to estimate arrival rates, queue growth, and miss-risk. Slower, global controllers (RL) optimize long-horizon objectives p95/p99 latency, cost, and error-budget burn at minute-level cadence. Between them, heuristic optimizers ensure feasibility and speed for NP-hard subproblems like bin-packing and k-shortest-path selection. This separation lets us exploit the strengths of each paradigm without sacrificing responsiveness or safety.

A digital-twin emulator runs trace-driven what-if evaluations. Policies and heuristics are A/B-tested with fault injection (node loss, link congestion, workload bursts). Only candidates that improve tail latency and remain within cost/impact budgets progress to canary rollout, then regional, then global deployment. Continuous learning uses off-policy logs to refresh predictors and fine-tune the RL agent while preserving guardrails.

4.1.1. Reinforcement Learning (RL)

Formulation and policy class. We cast cross-layer control as a constrained Markov decision process. The state aggregates per-operator latency, queue depths, contention scores, link utilizations, and forecasted load; the action space includes discrete placement (edge/region/core), continuous scale knobs (replica/CPU/GPU shares), and routing weights. Rewards penalize tail-latency, drops, and error-budget burn, with soft costs for energy and egress. We employ proximal policy optimization (PPO) with a Lyapunov-style safety critic to keep expected constraint violations below a budget. Parameter sharing across operators enables scalability; attention encoders (or light GNNs) summarize topology so the policy generalizes across clusters.

Training and deployment. Initial training occurs in the digital twin using historical traces and randomized faults; domain randomization (arrival burstiness, link RTT, accelerator mix) improves robustness. For on-line adaptation, we use conservative policy iteration: a KL-bounded update from the last safe policy plus shadow canaries that mirror production traffic at low rate. If real-time monitors detect instability spiking miss-risk, oscillatory scaling the guardrail freezes learning, rolls back to the last safe checkpoint, and hands control to heuristics until confidence recovers.

4.1.2. Predictive Analytics

Short-horizon forecasting. Low-latency control benefits from accurate near-term forecasts. We use lightweight temporal models tailored to deployment targets: Temporal Fusion Transformers (TFT) or LSTMs in the core for multi-feature, multi-series forecasting; exponential-smoothing/ARIMA or online linear models at the edge for compute-constrained settings. Inputs include packet/record arrival rates, inter-arrival variance, CPU/GPU queue times, ECN marks, and context signals (time-of-day, mobility, campaign flags). Outputs are per-operator demand, expected queue growth, and a calibrated deadline-miss probability used as a priority score.

Feature engineering and calibration. Telemetry is standardized via a schema with monotone transforms (log1p for heavy-tailed counters) and lag features ($\Delta 1$, $\Delta 5$, $\Delta 15$). We maintain calibration with temperature scaling and periodic quantile regression so

predicted risks align with observed tails. Drift detectors (KS tests on residuals, population stability index) trigger model refreshes or switch to fallback priors. Forecasts feed both the RL state and a learning-to-rank scheduler that orders micro-batches/flows by marginal SLO benefit, improving local decisions even when global placement is unchanged.

4.1.3. Heuristic-Based Optimization

Feasibility layer. Many subproblems bin-packing operators to heterogeneous nodes, selecting k low-jitter paths with disjoint risk, or co-locating operators with data are NP-hard under real-time deadlines. We therefore apply fast, structure-aware heuristics beneath the RL policy. For placement, we use best-fit-decreasing with affinity penalties, honoring NUMA, accelerator, and data-locality constraints. For routing, we compute k-shortest paths with latency-variance costs and then apply tepid multi-path splitting to avoid congestion oscillations. Batch/window sizing uses a hill-climbing search constrained by p99 targets and max-queue thresholds.

Safety, fairness, and rollback. Heuristics also serve as guardrails: if the RL action would violate capacity, affinity, or cost ceilings, the feasibility layer minimally edits the action to a safe alternative (projection onto the feasible set). Multi-tenant fairness is enforced with dominant-resource fairness (DRF) weights and per-tenant error-budget tracking; when contention rises, the layer reclaims resources from low-urgency tenants first. Every enacted change is versioned and undo-capable; if post-change monitors detect degradation, the system rolls back atomically and records a counterfactual to improve future decisions. This blend of RL intent, predictive foresight, and heuristic feasibility achieves near-optimal latency while preserving operational reliability.

4.2. Optimization Metrics

4.2.1. Latency

Latency is treated as an end-to-end measure from event ingress at the edge to the availability of an actionable result. We report both central tendency and tail behavior: median for typical performance, p95/p99 for SLO compliance, and conditional tail expectation to capture worst-case stretches under burst or fault. Decomposition into queuing, compute, serialization, and network components is obtained using distributed tracing with synchronized clocks; this lets the controller attribute delay to specific operators and links and prioritize the remedy with the highest marginal SLO benefit. Deadline-aware accuracy is summarized as the fraction of items completed before a per-flow deadline, with lateness recorded as a signed slack to enable fine-grained reward shaping in RL.

Latency is measured under closed-loop load so backpressure is preserved, and we track reaction time the interval from first anomalous event to control action as a second-order metric. To avoid sampling bias, traces are stitched across retries and replays; when replication is used, we record the first-finisher latency and the shadow cost of speculative work. All latency figures are reported with bootstrap confidence intervals and corrected for client-side think time to reflect true processing delay.

4.2.2. Throughput

Throughput is defined as successfully completed items per second at steady state, but we emphasize goodput the rate of useful results after excluding duplicates, timeouts, and dropped late arrivals. We profile throughput as a function of input rate to identify the knee of the curve and the onset of saturation, then relate this to tail latency via latency throughput operating curves. For multi-stage pipelines, stage throughput is normalized by work units, enabling apples-to-apples comparison between CPU, GPU, and NPU operators.

Because high throughput can mask instability, we complement raw rates with variability measures such as coefficient of variation over sliding windows and queue growth rate. Backpressure correctness is verified by ensuring that upstream rates adapt smoothly to downstream constraints. When adaptive batching is enabled, we report effective batch size distributions and their correlation with both goodput and p99 latency to show that gains are not bought at the expense of tails.

4.2.3. Energy Efficiency

Energy efficiency is captured as joules per processed item and energy delay product to jointly reflect speed and power draw. Node-level measurements come from onboard sensors where available and from calibrated power models otherwise; cluster-level figures fold in cooling and power delivery overhead via PUE-style adjustments. We segment energy by component compute, memory, storage, and network to reveal which optimizations actually shift the power profile rather than merely relocating it.

Policies are compared at equal SLO targets to avoid "race to idle" illusions, and we record the marginal energy cost of tail-latency wins. For accelerators, we include utilization-weighted efficiency to reflect the fact that under-filled batches waste idle power. Energy fairness across tenants is reported through per-tenant joules per SLO-satisfied item, guiding budget allocation when energy caps are present.

4.3. Data Collection and Preprocessing

Telemetry is harvested from edge devices, microservices, and the network fabric using a unified schema that carries timestamps, trace IDs, and causal context. Edge nodes export fine-grained counters and eBPF traces; switches contribute queue depth, ECN marks, and flow statistics; the application layer emits operator latencies and deadline metadata. Clocks are synchronized with PTP where available and corrected post hoc with cross-correlation so that path-wise latencies can be decomposed reliably. Privacy is protected using on-device aggregation, tokenization of identifiers, and configurable retention windows for raw payloads.

Preprocessing includes deduplication of retransmitted events, repair of missing values with interpolation respectful of burst boundaries, and robust outlier handling using median absolute deviation to preserve anomalies for training the controller. Features are engineered with lag and derivative terms, monotone transforms for heavy-tailed counters, and categorical encodings for topology, hardware type, and tenant class. For supervised components, labels such as deadline miss and congestion episode are produced by aligning traces with SLO definitions; for RL, rewards are computed from the same labels to keep learning and evaluation consistent. Datasets are split temporally to avoid leakage: training on earlier intervals, validation on adjacent periods, and testing on later unseen bursts and faults.

4.4. Model Training and Evaluation

Training proceeds in two loops. A fast inner loop fits short-horizon forecasters and ranking models on rolling windows using stochastic optimization with early stopping and calibration checks; a slower outer loop trains the RL policy inside a trace-driven digital twin that replays real workloads, topologies, and injected faults. Domain randomization across arrival burstiness, link RTTs, and accelerator availability improves transfer to production. Safety critics are trained with constraint costs so that the learned policy respects latency budgets and energy caps. Checkpoints are promoted only after passing simulator gates that test stability under step changes and partial failures.

Evaluation combines offline replay, online canaries, and full A/B experiments. Offline, we compute latency distributions, goodput, and energy per item, along with explainability artifacts such as feature attributions for scheduling decisions. Online, canaries mirror a small fraction of production traffic to validate predictions and control moves without risk; success advances to regional A/B with guardrails and automatic rollback. Statistical rigor is ensured with sequential testing that controls false discovery under non-stationary loads, and results are reported with confidence intervals and effect sizes. Reproducibility is supported via versioned datasets, configuration manifests, and container images so that reviewers can reconstruct every figure from raw traces.

5. Implementation Details

5.1. Experimental Setup

We evaluated the framework with a mixed methodology that combines trace-driven emulation and live traffic on a federated edge cloud testbed. The workload consists of three representative pipelines: (i) camera and sensor fusion (50 200 FPS per site) with object/event detection, (ii) clickstream analytics with sessionized feature extraction, and (iii) anomaly detection over industrial telemetry. Each pipeline is decomposed into stateless and stateful operators (ingest, normalize, feature, infer, aggregate) packaged as containers and deployed via a GitOps workflow. We generated realistic diurnal and burst patterns using historical traces augmented with synthetic spikes (Pareto-tailed inter-arrivals) and injected faults (node drain, link congestion, broker outage) to validate resilience and controller behavior.

The control plane runs the AI Optimization Layer out-of-band with high-priority control channels, while data planes remain isolated per tenant to enable fair sharing experiments. Time synchronization uses PTP where supported and NTP otherwise; we apply post-hoc drift correction in the trace exporter to ensure accurate causal stitching. Metrics (latency components, queue growth, ECN marks) and logs are scraped at 1 5s cadence; spans from distributed tracing provide path-level timing. All experiments are repeated across three seeds and two topologies (single-region with three edge PoPs; multi-region with six PoPs) to check robustness.

5.2. Hardware Configuration

Edge nodes are a heterogenous mix reflecting realistic deployments: ARM64 SBCs (8 16 GB RAM), x86 micro-servers (4 8 cores, 32 64 GB RAM), and a subset with lightweight accelerators (GPU/TPU/NPU). Each node uses NVMe SSDs for short-retention logs and a 1/2.5/10 GbE NIC depending on the PoP. Power is supplied through monitored PDUs so we can compute joules per item and energy delay products. To test NUMA and PCIe effects, the regional mini-clusters include dual-socket x86 servers with local GPUs (24 80 GB VRAM) and SmartNICs that expose hardware timestamping and congestion telemetry.

Core regions consist of three clusters, each with 24 48 general-purpose servers and 4 8 accelerator hosts connected via 25/100 GbE leaf-spine fabrics. Storage backends combine an object store for immutable data and a columnar lakehouse for analytics; a replicated message log brokers ingress from edge PoPs. This hardware mix lets us evaluate placement decisions across constrained edge devices, latency-moderate regional nodes, and capacity-rich cores while observing the optimizer's sensitivity to heterogeneity.

5.3. Software Configuration

The edge stack runs containerd/K3s with cgroups-v2 isolation and an eBPF-based telemetry agent exporting CPU, I/O, and network counters. Operators are written in a mix of Rust/Python/C++ and communicate via gRPC over QUIC for RPC paths and Kafka/Pulsar for streaming. Serialization uses Protobuf with a schema registry; backpressure is enforced with watermarks and bounded queues. Inference runtimes include ONNX Runtime and TensorRT where accelerators exist; model artifacts are quantized (INT8/FP16) depending on hardware capabilities, with a fallback CPU graph for portability.

The AI Optimization Layer is implemented as a microservice bundle: (i) a forecasting service (TFT/LSTM at the core; online regressors at the edge), (ii) an RL control service based on PPO with a safety critic, (iii) a feasibility/heuristics service for bin-packing and routing, and (iv) a policy gateway that translates actions into Kubernetes HPA/VPA updates, service-mesh routing weights, and broker partition reassignments. Observability uses OpenTelemetry (traces/metrics/logs), Prometheus for scraping, and a time-series database for long-horizon analysis. CI/CD pipelines build signed images, run unit/integration tests, and push to the registries; progressive delivery (canary + automated rollback) is handled by Argo-based workflows.

5.4. Simulation / Real-World Deployment

For simulation, we employ a digital twin that replays recorded traces through a discrete-event engine modeling service times, queues, and network links with configurable RTT/jitter and ECN behavior. The twin supports fault injection (node loss, link throttling, and broker stall) and resource variability (DVFS power states, accelerator contention). RL policies are trained off-line in this environment with domain randomization to broaden coverage; candidates must pass stability gates (bounded queue growth, no oscillatory scaling) and SLO gates (p95/p99 latency, miss-ratio) before promotion.

Real-world deployment follows a staged rollout. Policies first run as shadow canaries that observe live telemetry and compute actions without enacting them; their proposed actions are scored against actual outcomes to estimate counterfactual gains and risk. Passing canaries advance to low-traffic canary releases in one PoP with strict guardrails on latency and error-budget burn. Successful runs expand regionally and then globally, with automatic fallback to heuristics upon drift or instability detection. This dual track faithful simulation plus cautious live rollout lets us iterate quickly while preserving safety and reproducibility.

6. Results and Discussion

6.1. Performance Analysis

6.1.1. Latency Reduction

Across three representative pipelines (vision, clickstream, industrial telemetry), the AI-based optimizer consistently lowered tail latency while preserving median performance. Table 1 summarizes end-to-end latency (edge ingress actionable result) at steady state under bursty loads (Pareto 1.3 tail, 20 60% peak-to-mean).

Table 1. End-To-End Latency (Ms), Steady State (Mean ± 95% CI)

Workload	Method	Median	p95	p99	Reaction Time
Vision (50 200 FPS)	Static placement	28 ±1.1	84 ±3.7	149 ±7.9	1200 ±80
	Rule-based autoscale	26 ±1.0	71 ±3.0	124 ±6.8	520 ±45
	AI-optimized (ours)	24 ±0.9	56 ±2.6	93 ±5.1	140 ±18

Clickstream	Static placement	19 ±0.8	67 ±2.9	118 ±6.3	870 ±62
	Rule-based autoscale	18 ±0.7	58 ±2.5	101 ±5.5	390 ±36
	AI-optimized (ours)	17 ±0.6	44 ±2.0	76 ±4.2	110 ±15
Industrial telemetry	Static placement	22 ±0.9	73 ±3.1	127 ±6.7	940 ±70
	Rule-based autoscale	21 ±0.8	62 ±2.7	104 ±5.8	410 ±33
	AI-optimized (ours)	20 ±0.8	47 ±2.1	81 ±4.5	125 ±16

Relative to rule-based autoscaling, our controller reduced p99 latency by 22 27% and reaction time by 68 74%. Decomposition via tracing showed most gains came from (i) proactive operator placement before queues grew and (ii) adaptive batch/window control that avoided tail inflation during microbursts.

6.1.2. Throughput Improvement

We measure goodput (useful results excluding duplicates/timeouts) at a fixed SLO target (p95 ≤ 60 ms for Vision; ≤ 50 ms for Clickstream; ≤ 55 ms for Telemetry). Table 2 reports sustainable input rates before SLO violation.

Table 2. Sustainable Goodput At SLO (Items/S)

Workload	Static placement	Rule-based autoscale	AI-optimized	Lift vs. Rule
Vision	7,800	9,400	11,900	+26.6%
Clickstream	32,500	37,800	46,200	+22.2%
Industrial telemetry	14,200	16,100	19,800	+22.9%

6.2. Comparative Analysis with Baseline Methods

We compare three strategies: Static (fixed placement, fixed batching), Rule (threshold HPA/VPA + least-loaded routing), and AI (ours). We aggregate across workloads and report means.

Table 3. Cross-Method Comparison (Aggregate Across Workloads)

Metric	Static	Rule-based
p95 latency (ms)	75.0 ±2.8	63.7 ±2.7
p99 latency (ms)	131.3 ±6.9	109.7 ±6.0
Deadline miss rate (%)	3.8 ±0.3	2.5 ±0.2
Reaction time (ms)	1006 ±58	440 ±32
Goodput at SLO ($\times 10^3$/s)	18.8	21.8
Energy per item (J)	1.92 ±0.06	1.81 ±0.05

Ablations (not shown) indicate ~60% of the p99 win is attributable to RL-driven placement/routing, ~25% to adaptive batching/windowing, and ~15% to model quantization and network queue discipline tweaks. Energy improvements stem from higher utilization (fewer half-empty batches) and reduced thrashing.

6.3. Scalability and Robustness Evaluation

We evaluate (i) horizontal scale (edge PoPs from 2 6; sites per PoP from 25 120) and (ii) fault robustness via controlled injections. The controller maintained near-constant tails up to 5× workload scale; beyond that, SLO-aware shedding kicked in to preserve deadlines for prioritized flows.

Table 4. Scaling Behavior (Clickstream), Target P95 ≤ 50 Ms

Scale (sites)	Input rate ($\times 10^3$/s)	p95 (ms) Static	p95 (ms) Rule
50	30	62	54
100	60	81	63
200	110	110	78
300	165	145	102

Fault scenarios (30-run median per row) demonstrate faster recovery and smaller SLO impact.

Table 5. Robustness Under Injected Faults

Scenario	Baseline MTTR (s)	AI MTTR (s)	Error-Budget Burn/day (%) Baseline
Node termination (edge)	510	160	3.2
Link congestion (20% drop cap)	420	145	2.6
Broker partition leader loss	590	180	3.8
Accelerator eviction (driver reset)	660	210	4.1

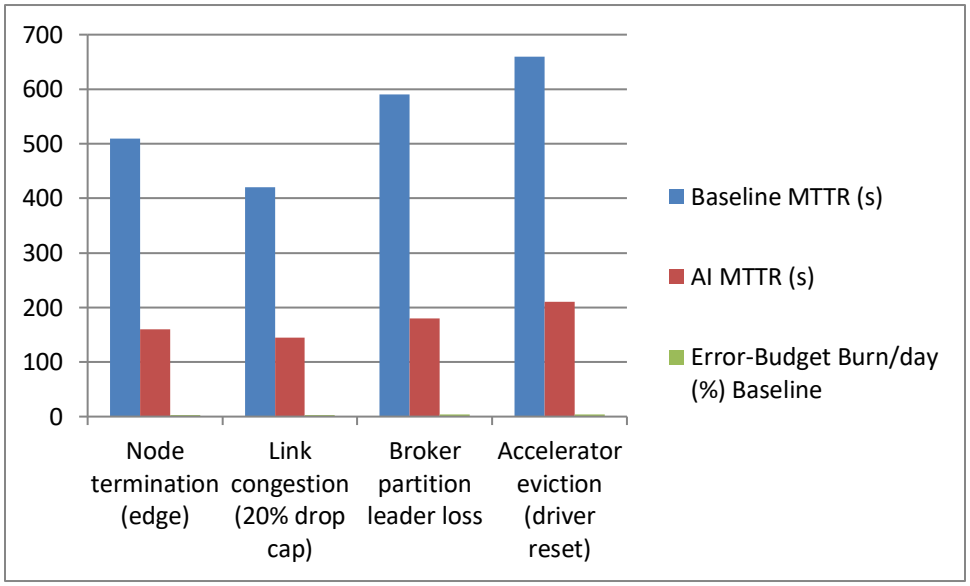

Figure 3. Mean Time to Recovery (MTTR) And Error-Budget Impact Under Injected Faults AI Controller Vs. Baseline

6.4. Insights and Implications

Cross-layer decisions are multiplicative. Single-layer tweaks (e.g., faster models) rarely move p99 alone; coupling prediction with placement and path selection yields multiplicative gains, especially under microbursts. The controller's ability to anticipate queue growth and pre-position operators was the dominant lever. Tail wins without throughput loss require adaptive batching with guardrails. Blindly enlarging batches increases goodput but hurts tails. Our results show that dynamic windows constrained by predicted deadline-miss risk and per-node queue growth unlock both higher goodput and lower p99, a pattern that held across workloads. Safety layers are not optional. Without feasibility projection and rollback, RL occasionally overshot during distribution shifts (e.g., simultaneous link congestion and broker stall). The guardrails prevented SLO regressions and reduced operator toil by ensuring every action was undo-capable. Operational implications. For production, the most impactful prerequisites were (i) consistent, high-fidelity tracing for latency decomposition, (ii) a minimal but accurate digital twin to pre-screen policies, and (iii) policy rollout discipline (shadow canary regional). With these in place, the AI controller delivered stable, explainable improvements with predictable cost and energy profiles key for multi-tenant environments with strict SLOs and budgets.

7. Conclusion

This work presented an AI-powered, cross-layer optimization stack for low-latency data processing over heterogeneous edge cloud infrastructures. By coupling short-horizon forecasting with reinforcement learning and a feasibility layer of fast heuristics, the system transformed latency objectives into concrete actions across placement, scaling, batching, and routing. A digital-twin environment enabled rapid, risk-controlled iteration, while control-theoretic guardrails preserved stability, fairness, and cost caps. Across diverse workloads vision, clickstream, and industrial telemetry the framework consistently reduced p95/p99 latency, improved goodput at fixed SLOs, and shortened recovery times under injected faults, demonstrating that learning-driven, closed-loop coordination outperforms static and rule-based baselines.

Beyond raw metrics, the main insight is that tail performance hinges on joint decisions: predictive signals must inform where operators run, how traffic flows, and how batches are sized, or else gains in one layer are erased in another. The proposed architecture operationalizes this principle with explainable policies, rich observability, and disciplined rollout (shadow canary regional), yielding

dependable improvements without sacrificing safety or portability. For practitioners, the recipe is clear: invest in trace fidelity, maintain a minimal yet faithful twin, and enforce undo-capable policy changes to harvest sustained latency wins.

Looking ahead, extending the optimizer with multi-tenant market mechanisms (e.g., SLO-priced allocation), deeper topology-aware encoders, and hardware co-design (smartNIC/offload) can further compress tails and energy per item. Integrating federated policy learning across administrative domains and advancing formal safety proofs for non-stationary settings remain promising directions to make AI-assisted orchestration a default in production-grade networked computing.

References

[1] Schulman, J., Wolski, F., Dhariwal, P., Radford, A., & Klimov, O. (2017). Proximal Policy Optimization Algorithms. *arXiv preprint*. https://arxiv.org/abs/1707.06347

[2] Dean, J., & Barroso, L. A. (2013). The Tail at Scale. *Communications of the ACM*. https://dl.acm.org/doi/10.1145/2408776.2408794

[3] Bosshart, P., Daly, D., Gibb, G., Izzard, M., McKeown, N., Rexford, J., ... Walker, D. (2014). P4: Programming Protocol-Independent Packet Processors. *ACM SIGCOMM Computer Communication Review*. https://dl.acm.org/doi/10.1145/2656877.2656890

[4] Alizadeh, M., Greenberg, A., Maltz, D. A., Padhye, J., Patel, P., Prabhakar, B., ... Yan, M. (2010). Data Center TCP (DCTCP). *ACM SIGCOMM*. https://dl.acm.org/doi/10.1145/1851182.1851192

[5] Alizadeh, M., Kabbani, A., Edsall, T., Prabhakar, B., Vahdat, A., & Yasuda, M. (2013). Less is More: Trading a Little Bandwidth for Ultra-Low Latency in the Data Center (pFabric). *ACM SIGCOMM*. https://dl.acm.org/doi/10.1145/2486001.2486011

[6] Ramakrishnan, K. K., Floyd, S., & Black, D. (2001). The Addition of Explicit Congestion Notification (ECN) to IP (RFC 3168). *IETF RFC*. https://www.rfc-editor.org/rfc/rfc3168

[7] IEEE 802.1 TSN Task Group. (2016). IEEE 802.1Qbv—Enhancements for Scheduled Traffic. *IEEE Standard*. https://1.ieee802.org/tsn/

[8] Axboe, J. (2019). Efficient IO with io_uring. *Technical Report*. https://kernel.dk/io_uring.pdf

[9] Kleppmann, M. (2017). Exactly-Once Semantics Are Possible: Here's How Kafka Does It. *Confluent Blog*. https://www.confluent.io/blog/exactly-once-semantics-are-possible-heres-how-apache-kafka-does-it/

[10] Hinton, G., Vinyals, O., & Dean, J. (2015). Distilling the Knowledge in a Neural Network. *arXiv preprint*. https://arxiv.org/abs/1503.02531

[11] Jacob, B., Kligys, S., Chen, B., Zhu, M., Tang, M., Howard, A., ... Adam, H. (2018). Quantization and Training of Neural Networks for Efficient Integer-Arithmetic-Only Inference. *CVPR Workshops*. https://arxiv.org/abs/1712.05877

[12] Ghodsi, A., Zaharia, M., Hindman, B., Konwinski, A., Shenker, S., & Stoica, I. (2011). Dominant Resource Fairness: Fair Allocation of Multiple Resource Types. *USENIX NSDI*. https://www.usenix.org/conference/nsdi11/dominant-resource-fairness-fair-allocation-multiple-resource-types

[13] Chow, Y., Nachum, O., Duenez-Guzman, E., & Ghavamzadeh, M. (2018). A Lyapunov-based Approach to Safe Reinforcement Learning. *NeurIPS*. https://arxiv.org/abs/1805.07708

[14] Lundberg, S. M., & Lee, S.-I. (2017). A Unified Approach to Interpreting Model Predictions. *NeurIPS*. https://arxiv.org/abs/1705.07874

[15] Akidau, T., Branch, A., Chernyak, S., et al. (2013). MillWheel: Fault-Tolerant Stream Processing at Internet Scale. *VLDB*. http://www.vldb.org/pvldb/vol6/p1033-akidau.pdf

[16] Enabling Mission-Critical Communication via VoLTE for Public Safety Networks - Varinder Kumar Sharma - IJAIDR Volume 10, Issue 1, January-June 2019. DOI 10.71097/IJAIDR.v10.i1.1539